LIDAR CAPABILITIES FOR MARTIAN DUST ANALYSIS

John F. Hahn[(1)] , Vladimir Podoba[(1)], Arkady Ulitsky[(1)], Diane Michelangeli[(2)] and Allan I. Carswell[(1)]

[(1)] Optech Incorporated, 100 Wildcat Road, Toronto, Ontario, Canada, M3J 2Z9 johnh@optech.ca; vladimirp@optech.ca; arkadyu@optech.ca; allanc@optech.ca
[(2)] York University, 4700 Keele Street Toronto, Ontario, Canada M3J 1P3 dvm@yorku.ca

ABSTRACT

Time of flight lidar data will provide new and useful information concerning dust and ice cloud distribution in the Martian atmosphere. The exact nature of the dust scattering environment is still under investigation at present.

The primary lidar observable is range-resolved atmospheric backscattering, most critically affected by scatterer number density and cross section. All estimates of the Martian dust number density and cross section are inferred from passive instrument observations, however, which depend upon scatterer complex refractive index and morphology. Because these parameter values are as yet not precisely determined, Martian dust size distribution resultant from the inversion of passive instrumentation is prone to wide interpretation [1,2,3,4].

In order to better prepare for Mars missions, terrestrial field studies have been undertaken and Martian dust analogs have been identified. Terrestrial field studies test lidar capabilities in Mars-like situations as well as cooperation between lidars and other instruments. Dust analogs provide a benchmark for study of Martian dust microphysical properties.

This paper evaluates Mars-related dust studies and their implications for lidar performance on Mars. Recommendations are made for terrestrial experiments with the view of better designing and interpreting lidar missions to Mars and matching lidar capabilities to the environment.

1. INTRODUCTION

The surface of Mars has been very cold and dry for eons. Although there is evidence of fluvial activity on Mars, the water is understood to be locked up as ice within a meter of the planet's surface, mostly in the northern hemisphere. The dry atmosphere and exposure to intense ultraviolet radiation and the pulverizing effect of meteorites has led to the development of dusty environment. The thin Martian atmosphere is in fact heavily laden with mineral dust compared to the terrestrial atmosphere and the greater part of the backscattered signal will be from dust and ice.

Martian dust storms and dust devils are significant features of Martian weather. From time to time dust storms envelop the entire planet in a single gigantic storm. In general, Martian dust storms are much larger than their terrestrial counterparts and are considered as potential hazards for manned mission, both on account of the wind as well dust as a hazard in its own right. From the experience of the Apollo missions, dust was found to tenaciously adhere to surfaces and vacuum seals.

Uncertainties in lidar performance are naturally offset by careful preparation, most especially consideration of the instrument capabilities within the presumed scattering medium. Scattering as governed by particle microphysical characteristics and the observation of macrophysical scattering phenomena are discussed from the point of view of Mars data. and from terrestrial field measurements and from these considerations recommendations for laboratory measurements can be.

2. MARTIAN DUST MICROPHYSICAL PROPERTIES

Martian dust has been weathered by intense solar ultraviolet radiation and micrometeorite bombardment for billions of years. The dust has been further weathered by entrainment and transport in dust storms and dust devils. These processes are among those that are viewed as making Martian dust properties rather different than Terrestrial mineral dusts.

Martian dust composition and morphological properties have been inferred from spectral observations of the Martian atmosphere from orbit with the Infrared Interferometer Spectrometer (IRIS) carried on Mariner 9 as well as the Infrared Thermal Mapper (IRTM) carried the two Viking orbiters. Surface based measurements of dust properties were also made from the Viking 1 and 2 Lander cameras and the Imager for Mars Pathfinder (IMP).

2.1 Martian Dust Composition

Mariner 9 IRIS Martian dust spectral data conformed well throughout the infrared to montmorillonite, a clay-like mineral. Absorption in the visible/ultraviolet as

reported by the Viking 1 and 2 and Pathfinder Landers, however, suggested the presence of another material. The evidence supports basaltic palagonite as the absorptive material. [5,6]. "Palagonite" is a generic term, describing more the physical condition of the material than its exact mineralogical composition but does imply a reduction in SiO_2 within the matrix of the mineral. Weathered palagonite is amorphous and pitted, with implications for optical extinction on Mars should the analogue be relevant there [1,7].

Table 1 compares the mineralogical composition of Martian dust with a standard terrestrial dust –Arizona Road Dust, a recognized industry standard for mechanical aging and wearing tests.

Table 1: ISO (Arizona) Test Dust Typical Chemical Analysis [8] and Anticipated Martian Basalt Dust Composition [9]

Mineral	Test Dust (% Weight)	Mars Dust (% Weight)
$Si0_2$	68 - 76	43.8
Al_20_3	10 - 15	10.1
Fe_20_3 (FeO)	2 - 5	(17.5)
Na_20	2 - 4	2.3
Ca0	2 - 5	5.3
Mg0	1 - 2	8.6
$Ti0_2$	0.5 - 1	0.7
K_20	2 - 5	0.7

The differences in composition affect the complex refractive index and absorption characteristics of the respective media. Martian dust particle size has been determined through passive instrumentation, and is consequently subject to uncertainty based upon unknowns in the scatterer complex refractive index and morphology [1,4,6]. Tomasko, *et al.* [2] reduced the number of free parameters required to describe scattering to five: the mean cross section-weighted particle radius, the mean cross section-weighted variance on the radius, the particle number density, the slope of the natural log of the phase function for internally transmitted light and the scattering angle at which the log of the phase function is minima. Scatterer morphology and composition affect the last two parameters.

Exposure of the dust particles to intense ionizing UV radiation and triboelectrification due to particle collisions may lead to electrostatic charging of the particles and perturbation of size distribution estimates [10,11,12,13]. The consequences of such a possibility, particularly in terms of particle aggregation with associated perturbation of particle size and shape estimates, bears a potentially large effect upon lidar performance.

2.2 Martian Dust Physical Attributes

The most critical physical attribute of dust with respect to lidar operation is its size distribution. However, size distributions were determined from inversion of passive instrument data that are affected by dust size, composition and morphology, with resulting variations in the derived size estimates.

Fig. 1 shows size distributions that have been derived from Viking and Mariner data. Three size distributions are shown. Dust size distributions 1 and 2 have modal values of 0.4 and 0.17 microns respectively and respective cross section weighted mean values of 1.7 and 1.2 microns. The third, derived by the authors of the paper, has a modal radius of less than 0.02 microns and and a cross section weighted mean value of 1.8 microns. This distribution was derived in order to provide the best match for the spectral data. The wide range in effective radii is due to the change in almost certainly imply widely varying lidar signal responses.

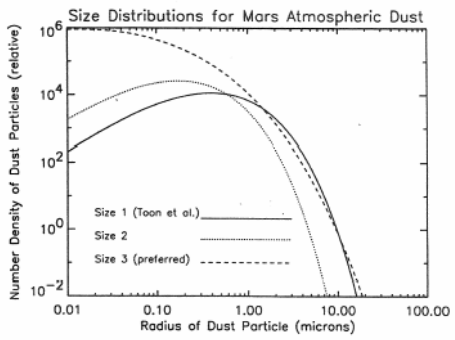

Fig. 1: Dust Particle Sizes Based upon the Modified Gamma Functions (from Clancy, *et al.* [1])

Other authors propose that a bimodal size distribution using similar dust composition breakdown yields the same spectral characteristics but without the very small modal values and also resembling dust size distributions also frequently found to be bimodal [14]

Thus, while field tests lend support to instrument characterization and shakedown, question concerning the particulars of the response may vary due to the optical properties resulting from the composition of the scattering medium.

2.3 Martian Dust Optical Properties

The physical properties of Mars dust were extensively modeled by Tomasko, *et al.* [2], from which scattering phase function were derived. Fig. 2 shows the results of their study, in which the total single scatter phase function is broken down into components. The results are for scattered light with a wavelength of 444 nm. The

particle effective radius is 1.6 microns with a variance to radius squared ratio of 0.2.

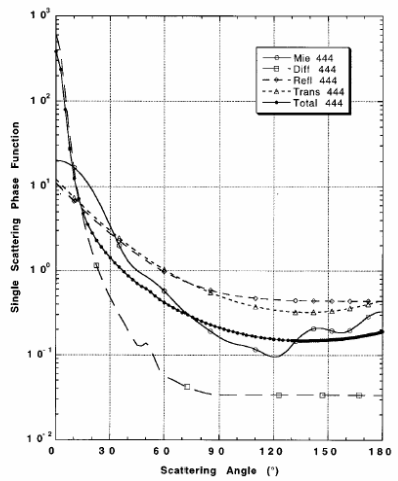

Fig. 2: Breakdown of Total Single Scattering Phase Function for Martian Dust (from Tomasko, *et al.* [2])

The results shown in Fig. 2 are derived from iterative calculations, using the observed spectral optical depth as a constraint. The figure provides a baseline for expected lidar backscattering strength, albeit one subject to the robustness of the retrieval.

3. FIELD TESTING OF LIDAR CAPABILITY

Lidars have been used since their inception in order to measure and characterize aerosols suspended in the atmosphere. More recently, lidar systems have worked cooperatively in networks such as EARLINET to trace and characterize atmospheric aerosols.

Lidar field tests have been performed with the specific intention of establishing lidar dust measurement capabilities in an approximately Martian context. The MATADOR field tests in 2001 at Eloy, Arizona explored among other things the use of lidars to detect and characterize dust devils. Two lidar systems were on site. Relevant parameters for the systems are listed in Table 2:

Table 2: Key Lidar System Parameters per MATADOR Field Study, 2001

Parameter	System 1: Optech ADC-1A	System 2: Optech ILRIS-3D
Pulse energy (mJ)	15	0.005
Pulse Frequency (Hz)	1	2000
Output Wavelength (μm)	1.064	1.535
Aperture (mm)	50	50
Scan rate (radian/sec.)	N/A	1.5

The ADC-1A uses a logarithmic amplifier in the signal processing electronics, affording the system an enhanced dynamic range in analogue detection mode. The ILRIS-3D is designed to provide rapid raster scans of a region with programmable horizontal and vertical scan angles, to create a 3-D point cloud of the reflecting targets in the field of view. A video camera is incorporated in this instrument for aiming and defining the area to be scanned. The output signals from the ILRIS were recorded on a flashcard disk for further processing. The two systems roughly enjoy the same optical power output.

An oscillogram screen capture from Lidar System 1 is shown in Fig. 3 [15]. The horizontal resolution is about 60 cm. The single-pulse return signal shows a double pulse return, indicating a walled structure in the dust devil. It is evident that the signal will become very large indeed at closer ranges.

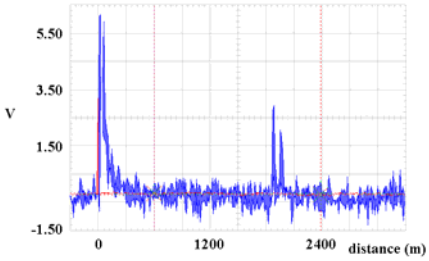

Fig. 3: Lidar signal return from a dust devil at about 2 m above the surface

System 2 was used to horizontally transect the dust devils. Fig. 4 shows the results of 29 scans collected within a 10-second interval through a dust devil. The point cloud is as seen from above. Only 6,000 out of 20,000 lidar shots fired were recorded, indicating that about two-thirds of the shots did not produce signals of sufficient intensity to reach the detection threshold. This may be of significance on Mars depending upon the characteristics of the dust environment there.

The point cloud reveals some of the internal structure of the dust devil. A number of filaments are visible towards the left of the distribution. Towards the right, the dust distribution is more condensed. At its widest, the dust devil has a line-of-sight width of about 10 meters. It is possible that the lidar return is showing the concentrated dust filaments as they are lifted up from the surface and spread throughout the dust devil volume.

These tests indicate the desirability of large dynamic range, large communication bandwidth and horizontal scanning capability in a Martian system. Large bandwidth and scanning capability, however, have power/mass and other penalties associated with them. A

simpler lidar system may very adequately be applied to a Mars mission, particularly if questions concerning the dust environment are carefully posed as hypotheses.

Additional lidar field tests are to take place in Eloy in the Spring of 2006.

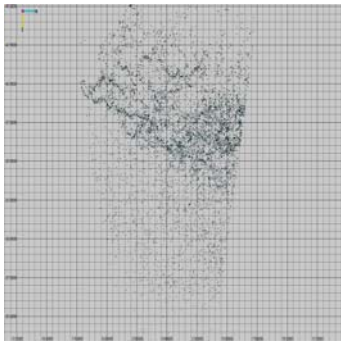

Fig. 2: Plan View of the System 2 Total Point Cloud Resulting from a Scan of a Dust Devil Moving from Left to Right in the Figure about 40 m from the Lidar

4. CONCLUSIONS

Simple lidar systems can be used to detect, track and characterize dust and clouds on Mars just as they have been used on Earth for decades. Scanning lidar systems can provide rich detail of information from a variable dust environment. Moreover, a variable dust environment speaks to the need of managing a variable return signal with a dynamic range of 90 dB on the returned optical signal.

Martian dust analogs can be used in the laboratory to simulate the Martian scattering environment. Analog materials of suitable compositional, size and weathering properties can be used in to simultaneously reproduce passive instrument results as lidar backscatter strength is measured. A library of results could then be built up providing a framework for the interpretation of mission data from Mars lidar instruments.

Laboratory sites have already been engaged in part for this type of work [16,17]

REFERENCES

1. Clancy, R. T., et al., *A New Model for Mars Atmospheric Dust Based upon Analysis of Ultraviolet through Infrared Observations from Mariner 9, Viking and, Phobos*, J. Geophys. Res. 100, pp 5251-5263, March 25, 1995

2. Tomasko, M. G., et al. *Properties if Dust in the Martian* Atmosphere *from the Imager on Mars Pathfinder*, J. Geophys. Res. 104, pp. 8987–9007 (1999)

3. Toon, O. B., et al. *Physical Properties of the Particles Composing the Martian Great Dust Storm of 1971-1972*, Icarus, 30, 663, 1977

4. Dlugach, Zh. M. and A. V. Morozhenko, *Parameters of Dust Particles in the Martian Atmosphere*, Sol. Sys. Res. 35, pp. 421–430, (2001)

5. Smith, P. H., et al., *Results from the Mars Pathfinder Camera*, Science, 278, pp. 1758–1765, December 5, 1997

6. Pollack, J. B., et al., *Viking Lander Image Analysis of Martian Atmospheric Dust*, J. Geophys. Res. 100, pp.5235–5250 (1995)

7. Morris, R. V., et al*., Phyllosilicate-poor Palagonitic Dust from Mauna Kea Volcano (Hawaii): a Mineralogical Analogue for Magnetic Martian Dust?* J. Geophys. Res. 106, pp. 5057–5083 (Mar. 2001)

8. Powder Technology Incorporated website: http://www.powdertechnologyinc.com/ docs/pages/product_list_4.html#arizona

9. NASA web site http://nssdc.gsfc.nasa.gov/planetary/ marspath/apxs_table1.html

10. Renard, J-B, et al., *Ultraviolet-visible Bulk Optical Properties of Randomly Distributed Soot*, Appl. Opt. 40, pp. 6575–6580 (Dec 2001)

11. Sternovsky, Z., et al., *Contact Charging of Lunar and Martian Dust Simulants,* Preprint

12. Stow, C. D., *Dust and Sandstorm Electrification*, Weather 24, pp. 134–140 (1969)

13. Farrell, W. M., et al., *Detecting Electrical Activity from Martian Dust Storms*, J. Geophys. Res. 104, pp. 3795–3801, Feb. 1999

14. Montmessin, F. P., et al., *New insights into Martian dust distribution and water-ice cloud microphysics*, J. Geophys. Res. 106, 5037, 2001

15. Renno, N. O., et al., *MATADOR 2002: A Pilot Field Experiment on Convective Plumes and Dust Devils*, Whitepaper prepared by the MATADOR Study Group, 2002

16. Renard, J-B, et al., *Light Scattering by Dust Particles in Microgravity: Polarization and Brightness Imaging with the New Version of the PROGRA2 Instrumen*t, Appl. Opt. 41, pp. 609–618, Feb. 2002

17. LSE (Light Scattering Experiment), The Netherlands Research School for Astronomy, http://www.strw.leidenuniv.nl/nova/instruments/LSE.html